

EFFECT OF CASTING SPEED AND TEMPERATURE ON SOLIDIFICATION OF DIRECT CHILL ALUMINIUM BILLETS UNDER THE INFLUENCE OF LOW FREQUENCY ELECTROMAGNETIC FIELD

HATIĆ Vanja¹, MAVRIČ Boštjan¹, KOŠNIK Nejc^{3,4}, ŠARLER Božidar^{1,2}

¹*Institute of Metals and Technology, Ljubljana, Slovenia, EU, vanja.hatic@imt.si*

²*University of Nova Gorica, Nova Gorica, Slovenia, EU*

³*Jožef Stefan Institute, Ljubljana, Slovenia, EU*

⁴*University of Ljubljana, Department of Physics, Ljubljana, Slovenia, EU*

Abstract

A model for simulation of direct chill casting under the influence of low frequency electromagnetic field was employed to calculate axisymmetric billet solidification under different casting parameters. Ten cases were calculated in order to study the combined effect of casting speed, casting temperature and external electromagnetic force on the melt flow and temperature distribution. All simulations are performed for the same geometry - an Al-5.25wt%Cu alloy billet with diameter of 288 mm. The model uses induction and conservation equations in order to model the coupled effect of electromagnetic field and melt flow. The spatial discretization is performed with a meshless diffuse approximate method. An explicit time stepping scheme was used. The macroscopic transport model results are subsequently used in two other independent models for solving the solid mechanics and microscopic grain growth equations.

Keywords: Casting Simulation, Direct Chill Casting, Low Frequency Electromagnetic Casting, Diffuse Approximate Method, Simulation of Casting Conditions

1. INTRODUCTION

Direct chill (DC) casting is a very popular technique for casting of light metals. It represents relatively simple process of billet production, where the molten metal is poured vertically. Initial heat is extracted through the mould in the primary cooling phase. Most of the heat is extracted in the second phase, where the water is sprayed directly on the billet surface. The process is prone to casting defects, such as porosity, hot tearing, surface defects and macrosegregation [1]. In addition to the alternation of the standard casting parameters, such as casting speed and temperature, a low frequency electromagnetic field (EM) can be induced in order to decrease the degree of casting defects. This additional EM body force can benefit several different properties of the semi-finished product. Among them are finer grain structure, decreased level of macrosegregation, elimination of macro porosity, etc. Until now, only one attempt of simulation of low frequency EM casting has been found in the literature [2], [3], where the geometry was a simple cylinder. A comprehensive model for simulation of DC casting under the influence of low frequency EM field has been developed at the Institute of Metals and Technologies (IMT) in recent years [4]. One of the main purposes of the model is to be able to simulate DC casting process for complex industrial inflow geometries. Only the macroscopic heat transport model is presented in the present paper. The model is also coupled with the solid mechanics and microscopic model, which are both presented in related publications [5], [6].

2. MODEL FORMULATION

A mixture continuum model was used to model the solidification process. The model assumes that the liquid and the solid phase are completely mixed. The mass, momentum, heat, and species conservation equations were first proposed and described by Bennon and Incropera in [7] and [8]. The assumption of constant and equal density was used in the model. The model was built in the cylindrical coordinate system (r, z, θ) . θ values

were not calculated due to the axial symmetry of the casting table geometry, boundary conditions, melt flow structure and temperature field. All the calculations were therefore performed in two dimensions (2D).

2.1. Navier-Stokes equations

The Newtonian fluid assumptions are used to model both solid and liquid phase as a pseudo-fluid. The effect of phase transition on the melt flow is modelled with Darcy's law for porous flow. With the use of the law we can model the packed solid particles as a rigid porous structure. The effect of free-floating equiaxed grains was not considered. The effect of turbulence was neglected due to the laminar flow assumption. The velocity of the solid phase is constant and equal to the casting speed \mathbf{v}_s . The mass and momentum transport equations for the mixture have the following form:

$$\nabla \cdot \mathbf{v} = 0,$$

$$\rho \frac{\partial \mathbf{v}}{\partial t} + \rho \mathbf{v} \cdot \nabla \mathbf{v} = -\nabla p + \mu \nabla^2 \mathbf{v} + \mathbf{b}_B + \mathbf{b}_{EM} + \frac{\mu}{K} (\mathbf{v}_s - \mathbf{v}). \quad (1)$$

\mathbf{v} is the velocity and p is the pressure of the mixture phase, t is the time, ρ is the mixture density and μ is the dynamic viscosity of the mixture. \mathbf{b}_B is a body force acting on the melt flow due to density changes. The buoyancy effect is considered with the use of Boussinesq approximation. The second body force, \mathbf{b}_{EM} , is the force due to effect of EM field. This force is calculated with the use of induction equation, which is described in section 2.3. The last term on the right hand side of momentum equation, represents the effect of the solid phase on the melt flow. An incremental fractional step correction scheme is used to ensure the mass conservation. The pressure correction term is obtained from Poisson equation. The pressure and velocity are then adjusted in order to obtain the incompressible flow solution.

2.2. Heat transport equation

The transport of heat is simulated with the mixture convection-diffusion equation:

$$\frac{\partial h_m}{\partial t} + \nabla \cdot (h_m \mathbf{v}) = \nabla \cdot \left(\frac{\lambda}{\rho} \nabla T \right) - \nabla \cdot [f_s (h_l - h_s) (\mathbf{v}_s - \mathbf{v})]. \quad (2)$$

The solid (h_s), liquid (h_l), and mixture (h_m) enthalpies are calculated with the following relations:

$$h_s = c_{ps} T,$$

$$h_l = c_{ps} T_{sol} + L_f + c_{pl} (T - T_{sol}), \quad (3)$$

$$h_m = f_s h_s + f_l h_l,$$

where c_{ps} and c_{pl} are the solid and the liquid heat capacity, respectively. L_f is the latent heat of fusion. The cooling process of the aluminium billet is simulated with different boundary conditions at the billet surface. This is performed with a variable heat transfer coefficient (HTC). Isolated conditions are assumed at the hot-top (HTC = 0 W/m²/K). HTC at the direct chill area depends on the cooling water flow rate, water and surface temperature. It includes effects of the film boiling, subcooled nucleation boiling and single phase heat transfer.

2.3. Electromagnetic field equations

The induction equation for \mathbf{A} is derived from the Maxwell equations:

$$\nabla^2 \mathbf{A} = \mu_0 \sigma \left(\frac{\partial \mathbf{A}}{\partial t} - \mathbf{v} \times \nabla \times \mathbf{A} \right) - \mu_0 \mathbf{J}_{ext}, \quad \phi = 0. \quad (4)$$

The equation is solved with an oscillating ansatz for the vector potential in order to obtain the complex-valued amplitude. The Lorentz force, which represents the direct influence of the EM field on the fluid flow of the

molten metal, is defined as a cross product of the current density (\mathbf{J}) and the magnetic field (\mathbf{B}), where Re represents the real part of a complex number:

$$\mathbf{b}_{Lorentz} = \text{Re} \mathbf{J} \times \text{Re} \mathbf{B} . \quad (5)$$

The time-averaged electromagnetic force calculated with equation (5) is used in the numerical solution of the Navier-Stokes equations.

3. MESHLESS NUMERICAL SOLUTION

A meshless diffuse approximate method (DAM) was used to solve the Navier-Stokes, heat transfer and EM field equations. A locally smooth and differentiable approximating function is constructed for discrete nodal information. The DAM uses weighted least squares to calculate the approximation [9]. The explicit time stepping scheme was used to perform the time integration.

3.1. Diffuse approximate method

Each computational node is assigned with its own subdomain due to localisation of the meshless procedure. The approximating function is determined for each subdomain n :

$$\hat{f}(\mathbf{x}) = \sum_{j=1}^m p_j(\mathbf{x}) \alpha_j = \mathbf{p}^T(\mathbf{x}) \boldsymbol{\alpha} , \quad (6)$$

where \mathbf{p} is a polynomial basis of dimension m and $\boldsymbol{\alpha}$ are the coefficients. The number of computational nodes in a subdomain must be greater or equal to the number of polynomial functions. The number of local nodes was equal to 14 in the simulations presented in this paper. The coefficients of the approximation are determined through the minimisation of the following expression:

$$J = \sum_{i=1}^n \theta(\mathbf{x}_i, \mathbf{x}) [f(\mathbf{x}_i) - \hat{f}(\mathbf{x}_i)]^2 , \quad (7)$$

where θ is the weighting function [10]. The weighting function has a maximum value in the central position of the subdomain and decreases with the Euclidian distance from the central position. The Gaussian function is frequently used as a weighting function and was also used in the simulations in this paper.

4. NUMERICAL EXAMPLES

Ten cases with different casting parameters were simulated. All of simulations were performed for the material properties of an Al-5.25wt%Cu alloy. The diameter of the aluminium alloy billet was equal to 288 mm. Plain casting table geometry with the hot-top, mould chill and direct chill was modelled. The casting table design is shown on **Figure 1**. Half of the simulations were performed for a conventional DC casting. Nominal values of casting speed (90 mm/min) and temperature (730 °C) were set in the first case. The casting velocity was modified in cases 2 and 3 to 80 and 100 mm/min, respectively. In addition, the casting temperature was varied in cases 4 and 5 to 720 °C and 740 °C, respectively.

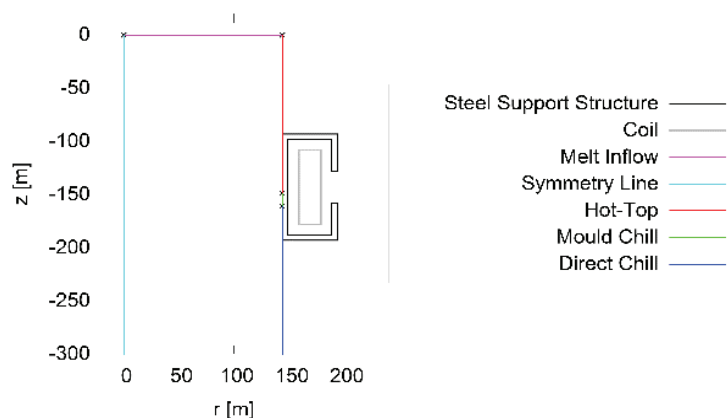


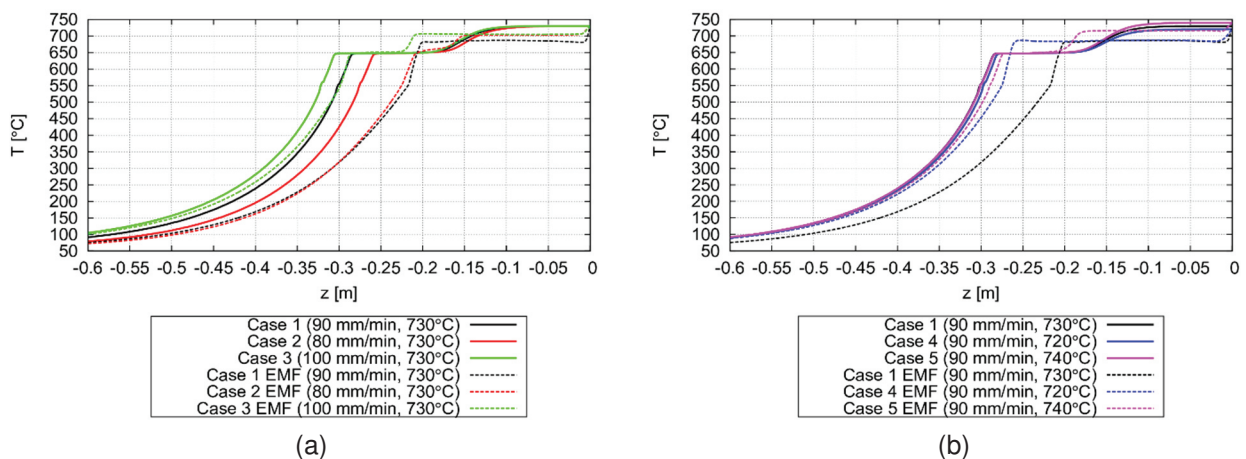
Figure 1 Geometry of the casting table used in simulations

The other half of the cases was simulated for the same casting parameters as the first part, yet the effect of low frequency electromagnetic field was also modelled. The intensity and frequency of the EM field were in all cases set to 100 A and 15 Hz, respectively. The position and the size of the coil and the support structure are shown on **Figure 1**, where the coil has 48 turns. The remaining casting parameters are given in **Table 1** and were identical for all cases. Approximately 20,000 computational nodes were used in each simulation case. A larger computational domain was used for computation of the Lorentz force, where approximately 210,000 computational nodes were used. Time step was set to 1×10^{-3} s.

Table 1 Material properties of Al-5.25wt%Cu alloy

T_{fusion}	660 °C	μ	$1.4 \cdot 10^{-3}$ kg/(m·s)	C_{ps}	1030 J/(kg·K)
$T_{solidus}$	643 °C	K_0	$5.79 \cdot 10^{-11}$ m ²	C_{pl}	1130 J/(kg·K)
$T_{liquidus}$	557 °C	ρ	2600 kg/m ³	λ_s	180 W/(m·K)
$k_{partition}$	0.173	L_f	377 kJ/kg	λ_l	80 W/(m·K)

Results are compared on **Figure 2**. The full, solid lines are used to show the results of conventional DC casting simulations. The dashed lines are used to show the results of low frequency EM casting simulations. All the results are plotted along the vertical centreline ($r = 0$). The temperature distribution is shown on (a) and (b). On (a) we can see that the increase of casting speed causes an increase in the billet sump. On (b) we can observe the effect of casting temperature; again we can see a well-known pattern that overheating causes increase the sump depth. Yet we are more interested in the effect of low frequency EM field on the results. The additional body force effects the temperature distribution in the desired way. The sump depth in the low frequency EM casting cases is smaller than in the DC casting cases for all the performed simulations. The effect of the EM force is even stronger in the case of smaller casting speed. The most profound effect was observed for the case 1, where the sump depth was decreased for approximately 8 cm. The Lorentz force has a favourable effect on the sump depth because the force is dominant in the horizontal direction and therefore intensifies the horizontal mixing. We can observe the horizontal component of the mixture velocity on **Figure 2** (c) and (d). The DC casting velocities are shown on (c) and low frequency EM casting velocities are shown on (d). The difference in velocity profiles is very large, as the magnitude is up to 50 times larger on plot (d). Also the distribution is different. The radial velocity on graph (c) is more or less constant at the hot-top region and is most intense in the sump. Yet, on (d) we can observe very intensive flow even in the hot-top area. The flow in the upper area has even larger magnitude than the flow in the sump. This is due to the large eddy formed in the vicinity of the mould. This eddy is driven by the Lorentz force, which increases the melt velocity in this area. A similar eddy structure is obtained in the simulations performed by other researchers [3].



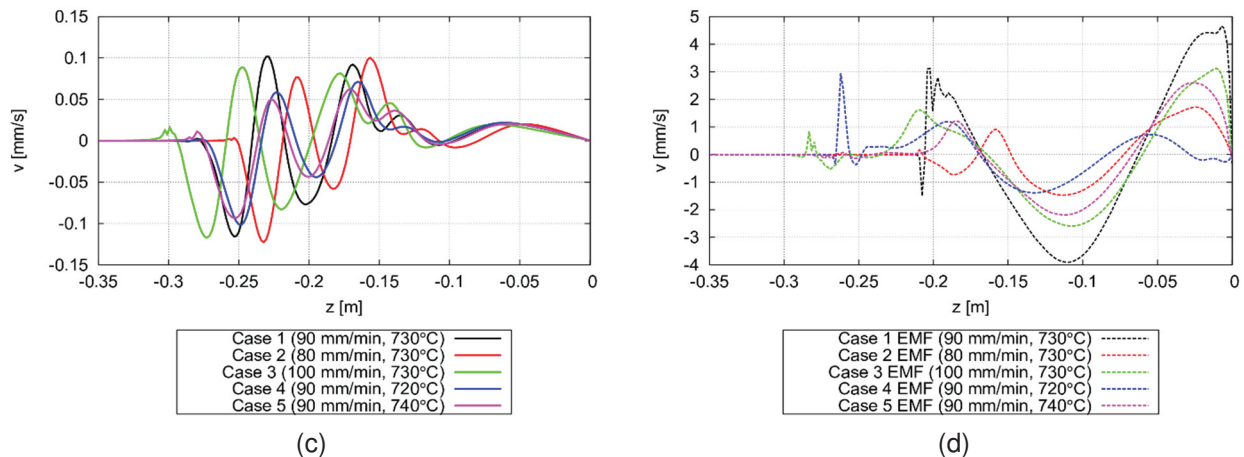


Figure 2 Results of the simulations in figures (a) and (b) show the temperature distribution at the centerline. The figures (c) and (d) show the radial velocity at the centerline

5. CONCLUSIONS

Effect of casting speed and casting temperature on the solidification of low frequency electromagnetic casting is investigated in this paper. A casting simulator, which was developed at the IMT with the cooperation of industry partner (Impol Casthouse), was used to make calculations under different casting parameters. The model is user friendly as it automatically generates node arrangement and the import of material properties is trivial. The spatial discretization was performed with a meshless DAM. The results have shown that the effect of EM field on the temperature field is large. Furthermore, the Lorentz force decreases the sump depth, which positively influences the semi-finished product quality. The effect is even more profound at low casting speeds. The result should be a smaller extent of macrosegregation, which will be simulated and investigated in the next stage of the research. The cause of the sump depth decrease is a more chaotic melt flow structure. The velocity component in the horizontal direction is up to 50 times larger in the cases calculated under the influence of EM field, which strongly increases the horizontal mixing process.

ACKNOWLEDGEMENTS

This work was supported by the Slovenian Research Agency and Impol Aluminium Industry under project L2-6775 Simulation of industrial solidification problems under influence of EM fields (NK & BŠ) and Young researchers programme (VH & BM).

REFERENCES

- [1] ESKIN, D.G. Physical metallurgy of direct chill casting of aluminum alloys. Boca Raton: CRC Press. 2008.
- [2] ZHANG, H., NAGAUMI, H., ZUO, Y., CUI, J. Coupled modeling of electromagnetic field, fluid flow, heat transfer and solidification during low frequency electromagnetic casting of 7XXX aluminum alloys: Part 1: Development of a mathematical model and comparison with experimental results. Materials Science and Engineering: A, 2007, vol. 448, pp. 189-203.
- [3] ZHANG, H., NAGAUMI, H., CUI, J. Coupled modeling of electromagnetic field, fluid flow, heat transfer and solidification during low frequency electromagnetic casting of 7XXX aluminum alloys. Materials Science and Engineering: A, 2007, vol. 448, pp. 177-188.
- [4] ŠARLER, B., GUŠTIN, A.Z., HATIĆ, V., KOŠNIK, N., MAVRIČ, B., VERTNIK, R. Simulation of multiscale industrial solidification problem under influence of electromagnetic field by meshless methods. In Coupled problems 2015. Barcelona: CIMNE, 2015, pp. 181-190.

- [5] MAVRIČ, B., ŠARLER, B. Modelling of stress fields during LFEM DC casting of aluminium billets by a meshless method. IOP Conference Series: Materials Science and Engineering, 2015, vol. 84, no. 012099.
- [6] KOŠNIK, N., GUŠTIN, A.Z., MAVRIČ, B., ŠARLER, B. A multiphysics and multiscale model for low frequency electromagnetic direct-chill casting IOP Conference Series: Materials Science and Engineering, 2016, vol. 117, no. 012052
- [7] BENNON, W.D., INCROPERA, F.P. A continuum model for momentum, heat and species transport in binary solid-liquid phase change systems-I. Model formulation. International Journal of Heat and Mass Transfer, 1987, vol. 30, pp. 2161-2170.
- [8] BENNON, W.D., INCROPERA, F.P. A continuum model for momentum, heat and species transport in binary solid-liquid phase change systems-II. Application to solidification in a rectangular cavity. International Journal of Heat and Mass Transfer, 1987, vol. 30, pp. 2171-2187.
- [9] VERTNIK, R., ZALOŽNIK, M., ŠARLER, B. Solution of transient direct-chill aluminium billet casting problem with simultaneous material and interphase moving boundaries by a meshless method. Engineering Analysis with Boundary Elements, 2006, vol. 30, pp. 847-855.
- [10] VERTNIK, R., ŠARLER, B. Solution of a continuous casting of steel benchmark test by a meshless method. Engineering Analysis with Boundary Elements, 2014, vol. 45, pp. 45-61.